Automatic Detection of Landslides from SAR Images: Application to the 2011 Kii Landslides

Masumi Yamada[1], Manabu Hashimoto[2], Yo Fukushima[3], Yuki Matsushi[4], Masahiro Chigira[5]
[1] Disaster Prevention Research Institute, Kyoto University
Gokasho, Uji, 611-0011, Japan, masumi@eqh.dpri.kyoto-u.ac.jp
[2] DPRI, Kyoto University, hashimoto.manabu.7e@kyoto-u.ac.jp
[3] DPRI, Kyoto University, yofukushima@rcep.dpri.kyoto-u.ac.jp
[4] DPRI, Kyoto University, matsushi@slope.dpri.kyoto-u.ac.jp
[5] DPRI, Kyoto University, chigira@slope.dpri.kyoto-u.ac.jp

Abstract – We analyzed TerraSAR-X images and found a good combination of filters and enhancement technique for the automatic landslide detection. We were successfully able to suppress noise in the image, identified landslide signals, and classify landslides from other surface changes. With a parameter set focusing on the completeness of detection, we achieved 98 % of detection from landslide catalog, but we have 50 times more false detection. With another parameter set focusing on the accuracy of detection, we achieved 80 % of detection from the catalog, and the signal-to-noise ratio was 27 %. Users can easily change the parameters depending on user's requirement. Quick detection of a landslide occurrence is very important for prompt emergency information, rescue efforts, and mitigation of further damage such as collapse of a landslide dam. Our approach proposed here will contribute to the rapid assessment of landslide hazards.

I. INTRODUCTION

Large deep-seated landslides occurred in the Nara, Wakayama, and Mie prefectures of western Japan when Typhoon Talas passed through the region on September 3-4, 2011. Heavy rainfall, exceeding 2000 mm in the Kii peninsula, triggered these destructive landslides [1]. The surface area of the largest landslides is estimated as 37 ha, and at least 72 landslides with the area larger than 1ha (~ 0.1 million m^3) occurred [2]. The landslides caused 56 fatalities and further 32 deaths due to flooding or other hazards in the Kii peninsula [3,4]. The total loss is estimated as at least 124 billion yen (~ 1 billion euro) [5]. This is the second largest natural disaster in 2011 after the Tohoku-Oki earthquake and tsunami.

Compiling the landslide distribution was a serious issue, since the region is not very populated and the transportation system was destroyed by landslides. Quick detection of a landslide occurrence is very important for prompt emergency information, rescue efforts, and mitigation of further damage such as collapse of a landslide dam. In this paper, we analyzed SAR images and identified landslides by comparing the catalog selected from aerial photos and the result of field surveys. We constructed an automatic method to extract landslides from large images for quick detection after disasters [6,7].

II. DATA

We used 3 pairs of TerraSAR-X images acquired before and after the landslide sequence for the analysis. Fig.1 shows the coverage of the 3 image pairs and the distribution of the deep-seated landslides. The landslides outside of the coverage were removed from the analysis and in total 56 landslides were targeted.

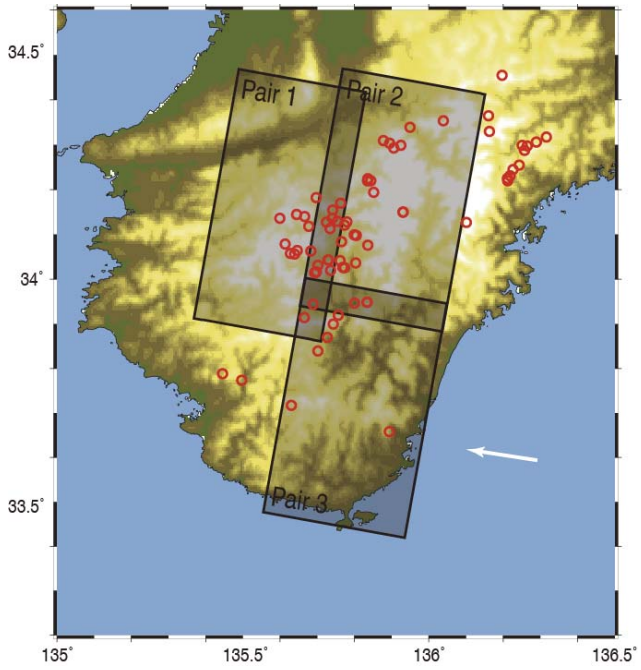

Fig 1. Distribution of the deep-seated landslides in Kii peninsula (red circles) and coverage of TerraSAR-X images (black rectangles). Arrows show the ground projection of the line-of-sight direction.

TerraSAR-X is a German satellite equipped with an active phased array X-band SAR antenna (wavelength 31 mm). The images were acquired from descending tracks with the strip-map mode with HH polarization. Local time of the acquisition was around 6 am. TerraSAR-X has about 0.9 ~ 1.4 m and 1.8 ~ 2.0 m resolutions in range and azimuth directions, respectively. The scene size is 30 km wide and 50 km long. Acquisition dates, incident angles, and perpendicular baseline lengths of the pairs are shown in Table 1.

We used the GAMMA software to process images. We used only coregistered and geocoded intensity images. ASTER Global Digital Elevation Model (GDEM) ver.2 were used for

geocoding. Finally, we converted intensity images into Sun-raster files.

The catalog of the deep-seated landslides was made by Public Works Research Institute (PWRI) [2]. The landslides with area of 1 ha or larger were extracted from aerial photos and the results of field surveys. We used the latitude, longitude, and area of each landslide for the evaluation of detection performance.

Table 1. Pairs of the images used in the analysis.

Pair	Master	Slave	Inc. ang. (deg)	B_{perp} (m)
1	2010/12/13	2011/11/19	39.3	23
2	2010/12/24	2011/10/06	37.5	-106
3	2010/12/24	2011/10/06	37.4	-105

III. METHOD

Intensity of the backscattered wave is sensitive to the roughness and slope of the ground surface. Due to the steep topography and forest vegetation in the Kii peninsula, the image pairs did not have enough coherence for interferometry. Therefore, we applied a color composite technique to intensity images to identify the location of landslides. We composed a single image by assigning intensities of the pre-event image to a red channel and those of the post-event image to green and blue (cyan) channels. We were able to identify more than 20 large landslides in the composite images visually. For the automatic detection of landslides from a SAR image, we need to suppress noise in the image, identify signals, and classify landslides from other surface changes. In this section, we explain a method to identify a landslide signal from the image efficiently.

A. Suppress noise in the image

We applied multiple filters and enhancement process to original intensity images to suppress noises and enhance signals. The original images include random noise and foreshortening zones (Fig. 2a). We tried to suppress the random noise and mask foreshortening zones.

First, a bilateral filter [8] was applied to reduce the random noise pattern (Fig. 2b). Pixels with intensity of outside of the measurement range, which results from the foreshortening, were masked (Fig. 2c) and median filter was applied to the image for reducing the high-frequency noise (Fig. 2d).

B. Identify signals in the image

Landslides change the vegetation of the ground surface and topography, which affects the backscattering of the SAR microwave. The roughness change of the surface from forest to rock surface makes the backscattering generally larger. The change in the angle between the incidence direction of the wave and the ground surface also changes the intensity of the back-scattered wave. Therefore, the change in intensity should clearly show the region of the landslides.

We computed the difference of the intensities of a pair raster image at each pixel. Pixels with intensity larger than a threshold were extracted and a binary image was created (Fig. 3a). In the image, small objects were filtered out by applying morphological closing on the binary image (Fig. 3b). To consolidate small objects close each other, we applied morphological opening on the image (Fig. 3c). We selected objects with area larger than a threshold and stored as identified signals (Fig. 3d).

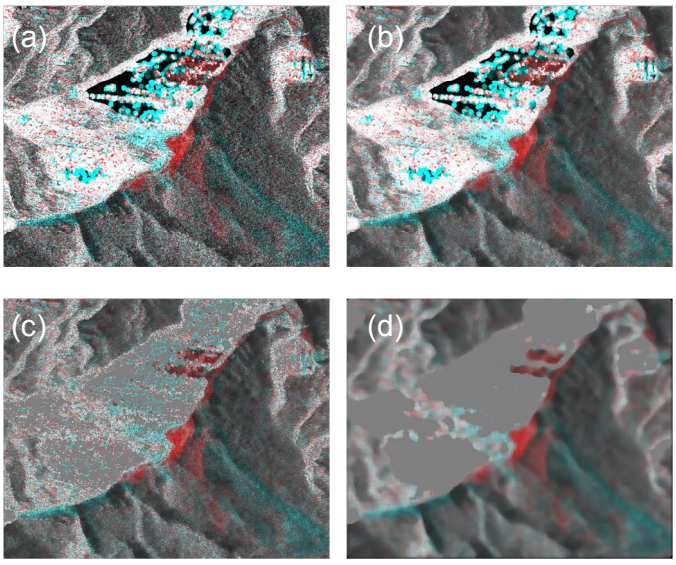

Fig 2. Example of the color composite image around Akatani landslide. Foreshortening zones are masked in gray on (c) and (d). See the text for details.

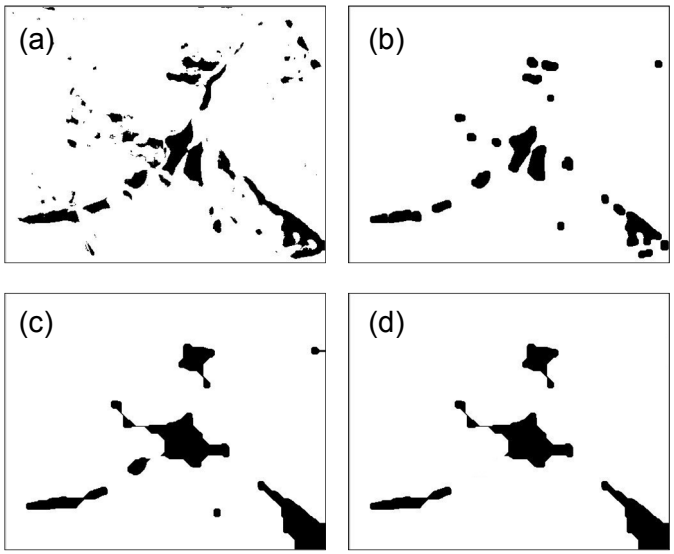

Fig 3. Example of the binary image around Akatani landslide. See the text for details.

C. *Classify landslides and others in the signals*

The identified signals include landslides and other changes. For example, deposits of debris flow, water level change of a river, and cutting of forest trees change roughness of ground surface, and the changes appear on the SAR image. Fig. 4 shows typical image of a landslide (a) and surface change on a river bank (b). The distribution of the color in a bounding box of an object is different. Fig. 4a includes both red and cyan pixels in the box, but cyan pixels are dominant in Fig. 4b. Therefore, we removed the objects on which one color occupied a certain percent of pixels. The threshold of percentage is optimized in the next subsection.

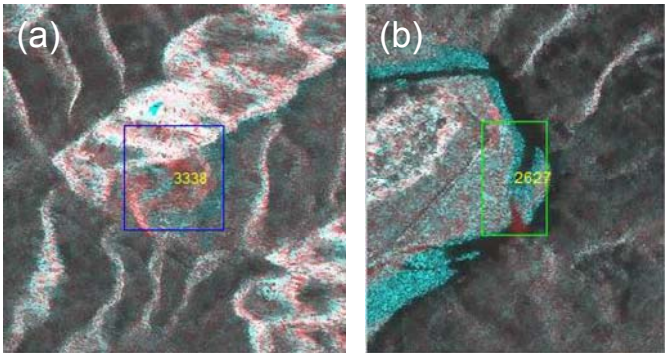

Fig 4. Example of the color composite image of a landslide (a) and debris on the river (b).

D. *Improving the performance of detections*

This detection method includes several parameters to control the performance of detections. We used 3 parameters (standard deviation of the bilateral filter, threshold of intensity for masking, and window size of the median filter) to control the effects of the filtering. To identify signals efficiently, 4 parameters (threshold for binarization, size of the morphological closing and opening, and threshold for the area) are used. A threshold of percentage of pixels with red or cyan color is also optimized. In total, we have 8 parameters to be optimized.

We optimized these parameters by comparing the detected objects with the landslide catalog of the PWRI. Considering the dimension of the landslide, we define the object as a landslide if the difference of the location is less than 0.7 km. We ran about 320 trials with different sets of 8 parameters, and found the parameter sets with the best performance of detection.

IV. Results and Discussions

An example of the composite image with filtering and identified events is shown in Fig. 5. Using the technique developed here, we were able to detect 45 landslides out of 56 landslides in the PWRI catalog for the most optimal case. We also identified several landslide dams where debris of landslides dammed up a river.

Fig. 6 shows the number of detected landslides and percentage of landslides over the total detected objects. There is a trade-off between the number of landslides and the accuracy of detection. As more landslides are detected, the accuracy decreases.

Here we explain the performance of two extreme parameter sets in Fig. 6 (A and B). The set A detected total 3086 objects and 2 % of them were landslides. The detection rate to the total number of landslides is 98 % (55/56). This set applies weaker filter on the image, and picks small landslide candidates. The signal-to-noise (S/N) ratio in the detected objects is not high, but it achieved a good completeness. This set will be appropriate for the case that the completeness is relatively important.

The set B detected total 167 objects and 27 % of them were landslides. The detection rate to the total number of landslides is 80 % (45/56). This set can detect relatively large landslide and small events may be missed. The area of smallest selected landslide is 1.1 ha, and the area of largest missed landslide is 13.1 ha (Imanishi landslide) which was not clearly observed in the composite image. This set will be useful for the case that the accuracy of detection is important.

We visually examined the objects detected by the parameter set B and not included in the PWRI catalog. Although most of the false detections were not landslides, some picked objects were confirmed to be a landslide in the aerial photos. They may be landslides smaller than 1 ha, which were not included in the PWRI catalog.

The parameter set can be changed depending on the user's purpose and the size of the target landslides. The performance of the detection may also depend on the image quality, image resolution and size of the landslides.

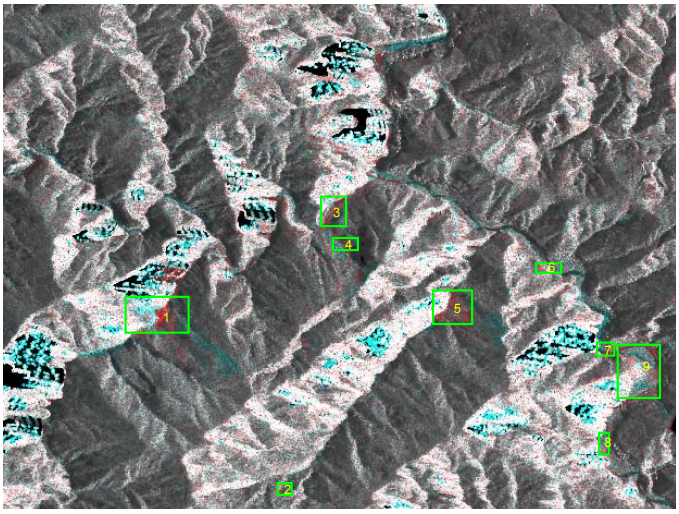

Fig 5. Example of the color composite image of landslides and results of the detection in green boxes.

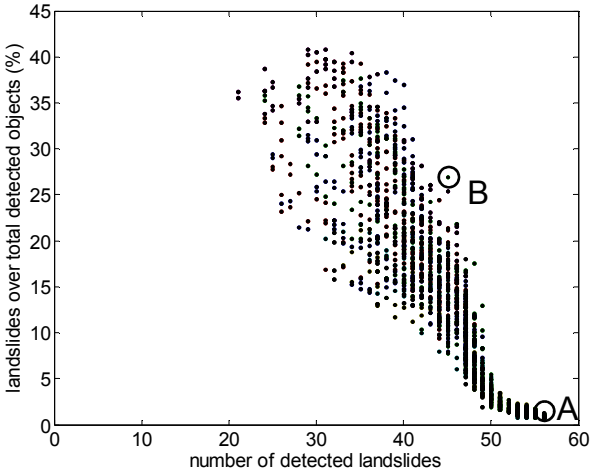

Fig 6. Number of detected landslides and percentage of landslide signals over total detected objects.

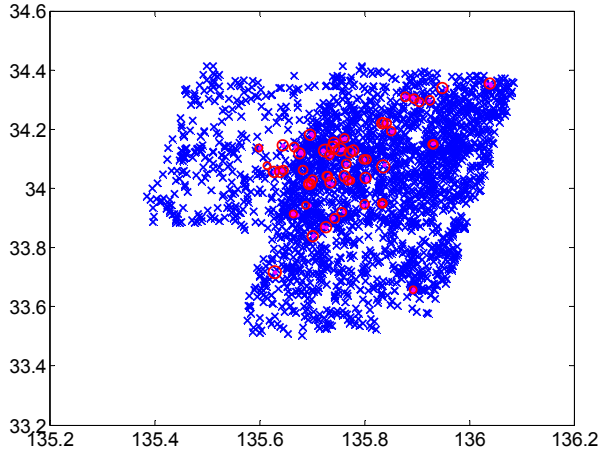

Fig 7. Distribution of the deep-seated landslides in the PWRI catalog (red circles) and all detected objects with the parameter set A (blue crosses).

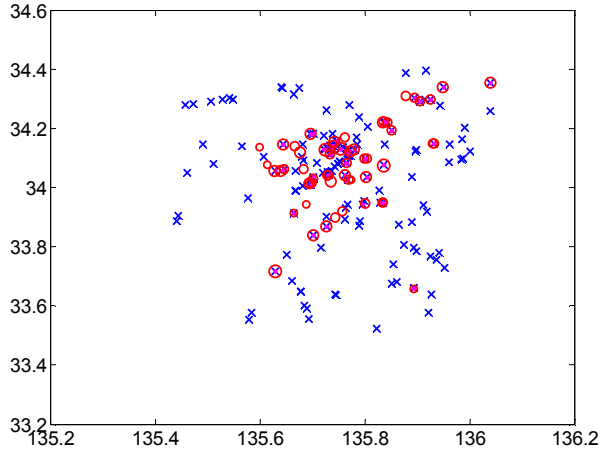

Fig. 8. Distribution of the deep-seated landslides in the PWRI catalog (red circles) and all detected objects with the parameter set B (blue crosses).

V. Conclusions

In this paper, we analyzed TerraSAR-X images and found a good combination of filters and enhancement technique for the automatic landslide detection. We were successfully able to suppress noise in the image, identified landslide signals, and classify landslides and other surface changes. With a parameter set focusing on the completeness of detection, we achieved 98 % of detection from PWRI landslide catalog, but we have 50 times more false detection. With another parameter set focusing on the accuracy of detection, we achieved 80 % of detection from the catalog, and the S/N ratio is 27 %. The behavior of the automatic detection system can be easily changed by changing parameters for different user requirement.

Quick detection of a landslide occurrence is important for prompt emergency information, rescue efforts, and mitigation of further damage such as collapse of a landslide dam. Currently, landslides are detected one by one looking at the color composite images manually. Our approach proposed here will reduce the time and effort for the detection and contribute to the rapid assessment of landslide hazards.

Acknowledgment

The authors would like to thank PWRI for providing list of deep-seated landslides in Kii peninsula. This research is funded by the PASCO CORPORATION.

References

[1] Yamada, M., Y. Matsushi, M. Chigira, and J. Mori, “Seismic recordings of the Landslides caused by Typhoon Talas”, Geophysical Research Letters, Vol.39, L13301, 2012.

[2] PWRI, http://www.pwri.go.jp/team/volcano/deep_seated_landslides/deep_seated_landslides_Typhoon12_2011.pdf

[3] NILIM report http://www.nilim.go.jp/lab/bcg/siryou/2012report/2012nilim20.pdf

[4] FDMA report http://www.fdma.go.jp/bn/%E5%8F%B0%E9%A2%A8%E7%AC%AC12%E5%8F%B7%E3%81%AB%E3%82%88%E3%82%8B%E8%A2%AB%E5%AE%B3%E7%8A%B6%E6%B3%81%E3%81%AB%E3%81%A4%E3%81%84%E3%81%A6%EF%BC%88%E7%AC%AC20%E5%A0%B1%EF%BC%89.pdf

[5] JA news, http://www.jacom.or.jp/news/2011/10/news111011-15118.php, Oct. 11, 2011

[6] Moine, M., A. Puissant, J. Malet, “Detection of landslides from aerial and satellite images with a semi-automatic method. Application to the Barcelonnette basin (Alpes-de-Hautes-Provence, France)”, Landslide processes - from geomorphologic mapping to dynamic modelling, 2009.

[7] Lei, L., Y. Zhou, J. Li; R. Burgmann, "Monitoring slow moving landslides in the Berkeley Hills with TerraSAR-X data," Geoscience and Remote Sensing Symposium (IGARSS), 2010 IEEE International , vol., no., pp.230,232, 25-30, 2010.

[8] C. Tomasi and R. Manduchi, "Bilateral Filtering for Gray and Color Images", Proceedings of the 1998 IEEE International Conference on Computer Vision, Bombay, India.